Biointerface Research in Applied Chemistry

www.BiointerfaceResearch.com

Evaluation of hepatoprotective and antioxidant activity of newly synthesized Ho(III) complex

Irena Kostova [1*], Ventzeslava Atanasova [1], Lozan Todorov [1], Magdalena Kondeva-Burdina [2], Virginia Tzankova [2]

[1]Department of Chemistry, Faculty of Pharmacy, Medical University, 2 Dunav Str., Sofia 1000, Bulgaria

[2]Laboratory "Drug metabolism and drug toxicity", Department "Pharmacology, Pharmacotherapy and Toxicology", Faculty of Pharmacy, Medical University, 2 Dunav Str., Sofia 1000, Bulgaria

*corresponding author e-mail address: **irenakostova@yahoo.com**

ABSTRACT

The holmium(III) complex was synthesized by reaction of the inorganic salt in amounts equal to ligand, molar ratio of 1: 3. The structure of the complex was determined by means of elemental analysis, FTIR and FTRaman spectroscopies. Detailed comparative vibrational analysis of the IR and Raman spectra of the complex with that of the free ligand (HAOA) allowed a straightforward assignment of the vibrations of the ligand groups involved in coordination. The binding mode in the complex was elucidated. The compounds HAOA and HoAOA were investigated for possible antioxidant activity in a model of non-enzyme-induced lipid peroxidation on isolated rat microsomes and for cytotoxicity on isolated rat hepatocytes. On isolated rat microsomes, administered alone, HAOA and HoAOA didn't revealed pro-oxidant effects, but in conditions of non-enzyme-induced lipid peroxidation showed antioxidant activity, which was stronger for the complex HoAOA. On isolated rat hepatocytes, isolated by two-stepped collagenase perfusion, both HAOA and HoAOA showed cytotoxicity, but complex HoAOA was with lower cytotoxicity then HAOA. We suggest that lower hepatotoxicity and higher antioxidant activity of the complex HoAOA, might be due to the presence of lanthanide ion in the structure of HoAOA.

KEYWORDS: *Holmium(III) complex; 5-aminoorotic acid; vibrational spectroscopy; hepatoprotective and antioxidant activity.*

1. INTRODUCTION

Lanthanide complexes are of great interest because of their numerous potential applications. Due to the unique nature of lanthanide ions the novel structures of lanthanide complexes possess special properties and offer great opportunities in terms of controlling their biological activity. The selection of suitable organic ligands along with different synthetic methods is a key step for the formation of lanthanide complexes with the desired features. It has been proved that ligands containing a combination of nitrogen and oxygen donor atoms are good building blocks for the formation of lanthanide coordination complexes. In recent years, the formation of coordination complexes between bioactive ligands having N, O/S donor binding sites and lanthanide(III) ions have received much attention because of their broad spectrum of biological, clinical, medicinal, agricultural, industrial, analytical and therapeutic applications. Orotic acid and its derivatives may therefore be good ligands for the construction of biologically active lanthanide complexes. Orotic acid (vitamin B[13]) and its salts and other derivatives play an important role in biological systems as precursors of pyrimidine nucleosides [1] and have been found in cells and body fluids of many living organisms [2–4]. Along with these compounds different metal complexes of orotic acid were studied [5–9]. The biological activity of orotic acid and its derivatives has been an area of great research ranging from bioinorganic to pharmaceutical and materials chemistry [10–12].

Because of the importance of orotic acid and its metal complexes in living systems, the coordination chemistry of orotic

acid has also been studied extensively [13, 14], including reliable assignments of their vibrational spectra [15, 16], theoretical investigations [16–27], interactions with other chemical species etc. Orotic acid is an interesting multidentate ligand capable of coordinating to metal ions through the nitrogen atoms of the pyrimidine ring, the two carbonyl oxygen atoms and the carboxylic group oxygen atoms, which results in a multi-faceted coordination chemistry depending on the conditions [28–31]. Thus, besides the biological relevance, the orotic acid and its derivatives are interesting multidentate ligands for the formation of metal coordination complexes with different structural features [32–37]. One of the most important derivatives of orotic acid is 5-aminoorotic acid (5-amino-2,6-dioxo-1,2,3,6-tetrahydro-pyrimidine-4-carboxylic acid, HAOA, Figure 1), which has relatively unknown coordination properties and has recently received attention in the field of medicinal chemistry [6, 38]. This ligand has demonstrated flexible coordination modes in formation of coordination frameworks. On the other side lanthanide(III) ions with their unique electron structure and large variety of valent states and coordination numbers are promising to form complexes with such organic molecules. The above considerations prompted us to obtain new Ln(III) coordination complexes with HAOA, especially in view of their application as antioxidant agents. For estimation of the most preferred reactive sites of HAOA for electrophilic attack and metal binding, its geometry was recently

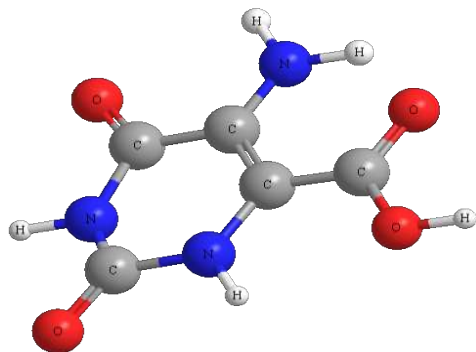calculated and optimized by us on the basis of DFT calculations [38].

Figure 1. Molecular structure of the ligand 5-aminoorotic acid (HAOA).

The present work can be regarded as a continuation of our efforts in the bioinorganic chemistry of lanthanide(III) complexes with a number of biologically active ligands. We have reported promising results on their significant cytotoxic activity in different human cell lines [39-48], which encouraged us to search for new lanthanide complexes. Thus, the aim of this work was to synthesize and characterize new holmium(III) complex of 5-aminoorotic acid and to evaluate its activity. In the present study 5-aminoorotic acid (HAOA) and its holmium(III) complex (HoAOA) were investigated for possible hepatotoxicity on rat hepatocytes, isolated by two-stepped, collagenase perfusion, and for possible antioxidant activity in a model of non-enzyme-induced lipid peroxidation on isolated rat liver microsomes, model of lipid membrane.

2. EXPERIMENTAL SECTION

2.1. Synthesis of the complex.

The compounds used were Sigma-Aldrich products, p.a. grade: $Ho(NO_3)_3.6H_2O$ and 5-aminoorotic acid. HAOA was used as a ligand for the preparation of the metal complex. The complex was synthesized by reaction of Ho(III) salt and the ligand, in amounts equal to metal: ligand molar ratio of 1: 3. The complex was prepared by adding an aqueous solution of Ho(III) salt to an aqueous solution of the ligand subsequently raising the pH of the mixture gradually to ca. 5.0 by adding dilute solution of sodium hydroxide. The reaction mixture was stirred with an electromagnetic stirrer at 25 °C for one hour. At the moment of mixing of the solutions, precipitate was obtained. The precipitate was filtered (pH of the filtrate was 5.0), washed several times with water and dried in a desiccator to constant weight. The obtained complex was insoluble in water, methanol and ethanol, but well soluble in DMSO.

2.2. Analytical and spectroscopic methods and instruments.

The carbon, hydrogen and nitrogen contents of the compound were determined by elemental analysis according to standard microanalytical procedures.

The solid-state infrared spectra of the ligand and its Ho(III) complex were recorded in KBr in the 4000-400 cm^{-1} frequency range by FT-IR 113V Bruker spectrometer.

The Raman spectra of HAOA and its new Ho(III) complex were recorded with a Dilor microspectrometer (Horiba-Jobin-Yvon, model LabRam) equipped with a 1800 grooves/mm holographic grating. The 514.5 nm line of an argon ion laser (Spectra Physics, model 2016) was used for the probes excitation. The spectra were collected in a backscattering geometry with a confocal Raman microscope equipped with an Olympus LMPlanFL 50x objective and with a resolution of 2 cm^{-1}. The detection of Raman signal was carried out with a Peltier-cooled CCD camera. The laser power of 100 mW was used in our measurements.

2.3. Pharmacology.

2.3.1. Reagents.

In our experiments, pentobarbital sodium (Sanofi, France), HEPES (Sigma Aldrich, Germany), NaCl (Merck, Germany), KCl (Merck), D-glucose (Merck), $NaHCO_3$ (Merck),

KH_2PO_4 (Scharlau Chemie SA, Spain), $CaCl_2.2H_2O$ (Merck), $MgSO_4.7H_2O$ (Fluka AG, Germany), collagenase from *Clostridium histolyticum* type IV (Sigma Aldrich), albumin, bovine serum fraction V, minimum 98 % (Sigma Aldrich), EGTA (Sigma Aldrich), 2-thiobarbituric acid (4,6-dihydroxypyrimidine-2-thiol; TBA) (Sigma Aldrich), trichloroacetic acid (TCA) (Valerus, Bulgaria), 2,2'-dinitro-5,5'-dithiodibenzoic acid (DTNB) (Merck), lactate dehydrogenase (LDH) kit (Randox, UK), $FeSO_4$ (Merck) and Ascorbinic acid (Valerus, Bulgaria), Glycerol (Valerus, Bulgaria) were used.

2.3.2. Animals.

Male Wistar rats (body weight 200-250 g) were used. The rats were housed in plexiglass cages (3 per cage) in a 12/12 light/dark cycle, under standard laboratory conditions (ambient temperature 20 ± 2° C and humidity 72 ± 4 %) with free access to water and standard pelleted rat food 53-3, produced according to ISO 9001:2008.

Animals were purchased from the National Breeding Centre, Sofia, Bulgaria. At least 7 days of acclimatization was allowed before the commencement of the study. The health was monitored regularly by a veterinary physician. The vivarium (certificate of registration of farm № 0072/01.08.2007) was inspected by the Bulgarian Drug Agency in order to check the husbandry conditions (№ A-11-1081/03.11.2011). All performed procedures were approved by the Institutional Animal Care Committee and made according Ordinance № 15/2006 for humaneness behaviour to experimental animals. The principles stated in the European Convention for the Protection of Vertebrate Animals used for Experiments and other Scientific Purposes (ETS 123) (Council of Europe, 1991) were strictly followed throughout the experiment.

2.3.3. Isolation of liver microsomes.

Liver is perfused with 1.15 % KCl and homogenized with four volumes of ice-cold 0.1 M potassium phosphate buffer, pH=7,4. The liver homogenate was centrifuged at 9 000 x g for 30 min at 4°C and the resulting post-mitochondrial fraction (S9) was centrifuged again at 105 000 x g for 60 min at 4°C. The microsomal pellets were re-suspended in 0.1 M potassium

phosphate buffer, pH=7.4, containing 20 % Glycerol. Aliquots of liver microsomes were stored at -70°C until use [49]. The content of microsomal protein was determined according to the method of Lowry using bovine serum albumin as a standard [50].

2.3.4. FeSO$_4$/Ascorbinic acid-induced lipid peroxidation *in vitro*.

As a system, in which metabolic activation may not be required in the production of lipid peroxide, 20 μM FeSO$_4$ and 500 μM Ascorbinic acid were added directly into rat liver microsomes and incubated for 20 min at 37°C [51].

2.3.5. Lipid peroxidation in microsomes.

After incubation of microsomes (1 mg/ml) with the compounds, we added to the microsomes 1 ml 25 % (w/v) trichloroacetic acid (TCA) and 1 ml 0.67 % 2-Thiobarbituric acid (TBA). The mixture is heated at 100°C for 20 min. The absorbance was measured at 535 nm, and the amount of MDA was calculated using a molar extinction coefficient of 1.56 x 105 M^{-1}cm^{-1} [51].

2.3.6. Isolation and incubation of hepatocytes.

Rats were anesthetized with sodium pentobarbital (0.2 ml/100 g). An optimized i*n situ* liver perfusion using less reagents and shorter time of cell isolation was performed. The method provided in higher amount of live and metabolically active hepatocytes [52].

After portal catheterization, the liver was perfused with HEPES buffer (pH = 7.85) + 0.6 mM EDTA (pH = 7.85), followed by HEPES buffer (pH = 7.85) and finally HEPES buffer containing collagenase type IV (50 mg/200 ml) and 7 mM CaCl$_2$ (pH = 7.85). The liver was excised, minced into small pieces, and hepatocytes were dispersed in Krebs-Ringer-bicarbonate (KRB) buffer (pH = 7.35) + 1 % bovine serum albumin.

Cells were counted under the microscope and the viability was assessed by Trypan blue exclusion (0.05 %) [53]. Initial viability averaged 89 %.

Cells were diluted with KRB to make a suspension of about 3 x 10^6 hepatocytes/ml. Incubations were carried out in flasks containing 3 ml of the cell suspension (i.e. 9 x 10^6 hepatocytes) and were performed in a 5 % CO$_2$ + 95 % O$_2$ atmosphere [53].

2.3.7. Cell incubation with HAOA and HoAOA.

Cells were incubated with concentration 100 μM of the complexes [54].

2.3.8. Lactate dehydrogenase (LDH) release.

LDH release in isolated rat hepatocytes was measured spectrophotometrically using a LDH kit [53].

2.3.9. Reduced glutathione (GSH) depletion.

At the end of the incubation, isolated rat hepatocytes were recovered by centrifugation at 4°C, and used to measure intracellular GSH, which was assessed by measuring non-protein sulfhydryls after precipitation of proteins with trichloroacetic acid (TCA), followed by measurement of thiols in the supernatant with DTNB. The absorbance was measured at 412 nm [53].

2.3.10. Malondialdehyde (MDA) assay.

Hepatocyte suspension (1 ml) was taken and added to 0.67 ml of 20 % (w/v) TCA. After centrifugation, 1 ml of the supernatant was added to 0.33 ml of 0.67 % (w/v) 2-thiobarbituric acid (TBA) and heated at 100°C for 30 min. The absorbance was measured at 535 nm, and the amount of TBA-reactants was calculated using a molar extinction coefficient of MDA 1.56 x 10^5 M^{-1}cm^{-1} [53].

2.3.11. Statistical analysis.

Statistical analysis was performed using statistical programme 'MEDCALC'. Results are expressed as mean ± SEM for 6 experiments. The significance of the data was assessed using the nonparametric Mann-Whitney test. A level of P < 0.05 was considered significant. Three parallel samples were used.

3. RESULTS SECTION

3.1. Chemistry.

Reaction of Ho(III) and 5-aminoorotic acid afforded a complex which was found to be quite stable both in solid state and in solution. The preparation of the Ho(III) complex is summarized in the next equations representing the dissociation of HAOA and the respective interaction of AOA$^-$ with Ho^{3+} ions:

$$HAOA \leftrightarrow H^+ + AOA^-$$

$$[Ho(H_2O)_n]^{3+} + 3AOA^- \rightarrow Ho(AOA^-)_3.H_2O,$$
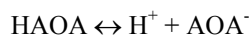
where HAOA = C$_5$N$_3$O$_4$H$_5$ и AOA$^-$ = C$_5$N$_3$O$_4$H$_4^-$.

The newly synthesized Ho(III) complex was characterized by elemental analysis. The content of the metal ion was determined after mineralization. The used spectral analyses confirmed the nature of the complex.

The data of the elemental analysis of the Ho(III) complex serve as a basis for the determination of its empirical formula (Ho(AOA)$_3$.H$_2$O) and the results are presented below, % calculated/found: C= 25.97/25.64; H= 2.02/2.29; N= 18.18/18.16; H$_2$O= 2.59/2.28; Ho= 23.81/24.15, where HAOA= C$_5$N$_3$O$_4$H$_5$ and AOA= C$_5$N$_3$O$_4$H$_4^-$.

The determination of the binding mode in the complex on the basis of physicochemical and spectroscopic methods, when crystal and molecular structure data are not available, is not a trivial task. The geometry of HAOA and of the model La(III)-AOA was computed and optimized by us with the Gaussian 03 program employing the B3PW91 and B3LYP methods with the 6-311++G** and LANL2DZ basis sets [38]. Theoretical simulations of vibrational spectra for the model La(III)-AOA complex and a comparison with the experimental ones were very helpful for extracting reliable structural information on the newly synthesized Ho(III) complex [38]. In the present study the binding mode of the HAOA ligand to Ho(III) ions was elucidated by recording the vibrational spectra of the complex in comparison with those of the

free ligand. It was found that the density functional theory (DFT) calculated geometries, harmonic vibrational wavenumbers including IR and Raman scattering activities for the ligand and its La(III) complex [38] were in good agreement with the experimental data for the Ho(III) complex.

3.2. Vibrational spectroscopy.

Because no X-ray crystal structure data were available for the ligand HAOA, its structure was optimized for the first time at different levels of theory by us [38] and compared with literature data for similar compounds like orotic acid obtained by X-Ray diffraction. It was found that the existence of intramolecular hydrogen bonding is highly probable in the calculated solid state conformation of HAOA [38]. There are several modes of particularly strong intramolecular hydrogen bonding for HAOA, which take place between the coordinated carboxylate O1 and one of the protons of amino group, between the pyrimidine carbonyl oxygens O4 and the other one of the protons of amino group, and between the carboxylate O3 and the imido N1-H1 group (Figure 1). These intramolecular hydrogen bonds play an important role in the crystal packing and their influence on the respective vibrational IR and Raman spectra has been taken into consideration.

The optimization of the geometry of La(III) complex of 5-aminoorotic acid with B3PW91/LANL2DZ and B3LYP/LANL2DZ methods [38] revealed that HAOA coordinated to La(III) as a dianion and the complex contained three HAOA ligands. It has been found that 5-aminoorotic acid binds to the La(III) ion through both oxygen atoms of the carboxylic group from all three ligands; the central atom La(III) is six-coordinated and form together with the ligands a trigonal prismatic structure [38]. It should be stated that different hydrogen bonds were observed in the calculated La(III) complex of HAOA [38]. The theoretical study performed by us earlier has helped us to interpret properly the vibrational IR and Raman spectra of the newly synthesized Ho(III) complex.

The vibrational spectra, presented in Figs. 2 and 3, were analyzed by comparing the respective modes with those from the literature [55-57] and in combination with the results of our DFT calculations (i.e., harmonic vibrational wavenumbers and their Raman scattering activities) [38]. The selected experimental IR and Raman data of the ligand and the newly synthesized Ho(III) complex and their tentative assignments are given in Table 1.

The vibrational spectra of HAOA and its Ho(III) complex are relatively complex (Figs. 2 and 3). Several contributions of relatively high IR intensity were found, corresponding to carbonyl, carboxylic and C=C stretching, and amino bending vibrations, which appear strongly coupled and their assignment was quite difficult because of the involvement of these groups in hydrogen bonds which affected their wavenumbers and produced a relevant band broadening as per the literature reports [38, 55-57].

In the 2000-3500 cm^{-1} spectral region the O-H, N-H, and C-H stretches give rise to intense IR bands (Figure 2, Table 1). The assignment of the O-H and N-H stretching bands is rather difficult. These bands appear overlapped in the same spectral region, and the involvement of these groups in hydrogen bonds affects their wavenumbers and produces a relevant band broadening in the IR and Raman spectra.

In the ν(OH)$_{water}$ region the IR spectrum of Ho(III) complex shows one medium band at 3448 cm^{-1}, attributed to the presence of coordinated water [58]. This band overlaps with the ν_{asym}(NH$_2$) band [57]. The ν(N–H) stretching wavenumbers in HAOA appear little affected due to the intermolecular H-bonds. In the IR spectra, the strong band at 3457 cm^{-1} (HAOA) and the band at 3448 cm^{-1} (Ho(III) complex of HAOA) were assigned to the N1-H1 stretching modes from the pyrimidine rings (Table 1), while the bands at 3333 cm^{-1} in the IR spectrum of HAOA as well as the band at 3332 cm^{-1} from the IR spectrum of Ho(III) complex of HAOA were attributed to the N3-H3 stretching modes (Figure 2, Table 1).
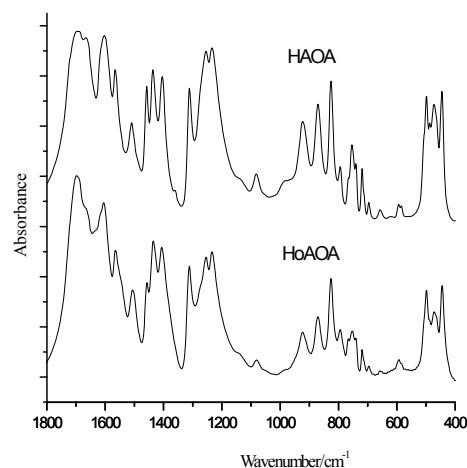

Figure 2. IR spectra of 5-aminoorotic acid (HAOA) and its Ho(III) complex.
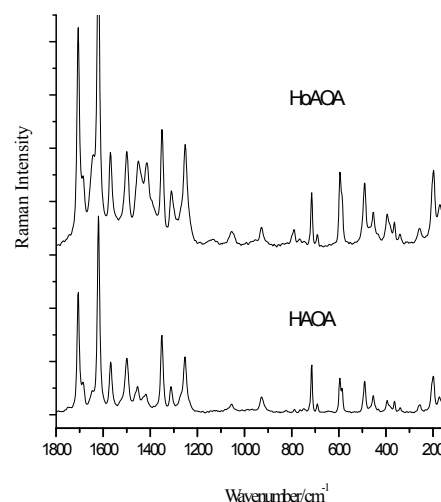

Figure 3. Raman spectra of the solid state of 5-aminoorotic acid (HAOA) and its Ho(III) complex. Excitation: 514.5 nm, 100 mW.

The Raman spectra of the free 5-aminoorotic acid and of the complex, shown in Figure 3, revealed dramatic intensity changes in going from the acid to the complex (Table 1). In the Raman spectra, the N3-H3 stretching vibrations are present for the ligand and for the complex (Table 1, Figure 3). The NH$_2$ asymmetrical stretching mode that is absent in the IR and Raman spectra of the ligand can be seen in the IR and Raman spectra of the complex at 3355 cm^{-1} as a medium band (IR) and 3357 cm^{-1} as a weak band (Raman), whereas the symmetrical NH$_2$ stretch is

present in both IR spectra by bands with medium relative intensity at 3196 and 3170 cm^{-1} and in Raman spectrum of the ligand as a very weak band at 3166 cm^{-1}.

Moreover, the wavenumber region 2700-3000 cm^{-1} in the IR spectra of HAOA and its Ho(III) complex is typical of strongly hydrogen bonded intermolecular complexes due to a strong anharmonic coupling (Fermi resonance) of the N-H stretching vibrations with overtones and combinations of lower frequency modes of the bonded molecules [38].

The C=O groups are very important as they take part in hydrogen bonding, especially in nucleic acid base derivatives. When the carbonyl is hydrogen bonded but not dimerized, a bond active in the IR spectra appears at about 2700-3000 cm^{-1} and also another bond active in both IR and Raman spectra appears at 1730-1705 cm^{-1} [38]. In our IR spectra these bands with medium and weak intensities for the ligand and the complex, respectively, can be observed at 2850 and 2831 cm^{-1}. Besides, one very strong band can be observed in 1730-1690 cm^{-1} region at 1691 cm^{-1} in the IR spectrum of the ligand and one medium band at 1703 cm^{-1} in the IR spectrum of the complex, which were assigned to the symmetrical stretching mode of C2=O2 (Figure 2). Opposite to the IR spectra, in this region of the Raman spectra only a medium band at 1699 cm^{-1} for the free ligand was observed. It is detected that the ν(C2=O2) band's position remains almost unaffected by changes in the molecular structure of the uracil ring. This is caused by the fact that the C2=O2 group is quite distanced from the COOH and NH$_2$ groups and, moreover, it is surrounded by the two N–H groups, which buffer it from influences of the remaining molecular moieties [38]. On the other hand, the C4=O4 moiety is nearer to the NH$_2$ group, and due to an intramolecular contact between both, the N–H and C4=O4 bonds appear slightly lengthened. The dimer form is best characterized by the Raman bands in the 1680-1640 cm^{-1} range [38] and by IR bands, around 1290 cm^{-1} and between 1440 cm^{-1} and 1395 cm^{-1} (C-O stretching mode) (Figs. 2 and 3; Table 1). The strong band at 1667 cm^{-1} from the IR spectrum of HAOA and the two very strong bands at 1699 cm^{-1} and 1679 cm^{-1} from the IR spectrum of the complex, were assigned to the symmetrical stretching modes of C4=O4 and to the asymmetrical COO$^-$ stretching modes. In the Raman spectra, these vibrations can be observed as a shoulder at 1678 cm^{-1} for the ligand and as a medium band at 1705 cm^{-1} for its Ho(III) complex (Table 1, Figs. 2 and 3). When the protons of –NH$_2$ group are

engaged in intramolecular hydrogen bonding, the electron lone pair of the N atom is coupled more readily with the π-electrons of the C5=C6 bond. In the IR spectra of HAOA and its Ho(III) complex, the strong and very strong bands at 1604 and 1608 cm^{-1}, respectively, were attributed to the C5=C6 stretching contributions, NH$_2$ scissoring and ν(COO$^-$) vibration [38, 59], whereas in the Raman spectra these vibrational modes are distinguish through the very strong bands at 1612 cm^{-1} for the ligand, and at 1621 cm^{-1} for its Ho(III) complex. An increase in the ν(C=C) wavenumber in the ligand appears related to an increment in the negative charge on substituent in position 5.

The medium bands from the IR spectra at 1566 cm^{-1} (ligand) and 1554 cm^{-1} (Ho(III) complex), as well as the medium peaks from the Raman spectra at 1560 cm^{-1} (ligand) and 1568 cm^{-1} (Ho(III) complex), were attributed to the C5=C6 stretching and in plane N-H bending modes (Table 1). The next pyrimidine ring vibrations, as N-C and N-H bending modes, can be observed in the 1520-1490 cm^{-1} wavenumber region (Table 1, Figs. 2 and 3). In the IR spectra, the medium band at 1312 cm^{-1} for HAOA as well as the medium signal at 1309 cm^{-1} for the complex were attributed to the C5–N stretching modes (Figure 2), while in the Raman spectra these vibrations can be observed as a weak peak at 1301 cm^{-1} for the ligand and as a medium/strong signal at 1310 cm^{-1} for the complex and they are shifted to lower wavenumbers (Table 1, Figure 3).

The Raman bands at 425 and 249 cm^{-1} (HAOA) and at 435 and 255 cm^{-1} (Ho(III) complex of HAOA) were assigned as Δ_{as}(COO) and Δ_s(COO) modes, respectively. The symmetrical COO$^-$ stretching mode was observed in the IR spectra as medium and strong bands at 1405 and 1377 cm^{-1} for the ligand and its Ho(III) complex, respectively, while in the Raman spectra this vibration appears as a strong peak at 1351 cm^{-1} only for the complex (Figs. 2 and 3). In general, we could assert wavenumbers shifting, increasing and/or decreasing in relative intensities, as well as appearances and/or disappearing of bands comparing the IR and Raman spectra of the ligand and of the metal complex. The metal affects the Ho-O bonds and this effect is transferred to the C-O bonds. The pyrimidine ring bending vibration and the skeletal deformation bands of the free ligand (900-300 cm^{-1}) show considerable changes on complex formation (Figs. 2 and 3; Table 1). These changes may be attributed to distorsion of the pyrimidine rings upon complexation.

Table 1. Selected experimental IR and Raman wavenumbers (cm^{-1}) of 5-aminoorotic acid (HAOA) and its Ho(III) complex and their tentative assignments

IR		Raman solid		Vibrational assignments
HAOA	HoAOA	HAOA	HoAOA	
3457 s	3448 w	3456 vw		ν(N1H1)
	3355 m		3357 w	ν_{as}(NH$_2$)
3333 s	3332 m	3323 m	3333 w	ν(N3H3)
3196 m	3170 m	3166 vw		ν_s(NH$_2$)
2850 w	2831 w			Bonded NH$\cdots$O
1691 vs	1703 m	1699 m		δ(NH); ν_s(C2=O2), ν(Nl–C6)
	1699 vs			ν_s(C4=O4)
1667 s	1679 vs	1678 sh	1705 m	ν_s(C4=O4); ν(COO$^-$), ν(C5=C6), δ(N3–H3)

1604 s	1608 vs	1612 vs	1621 vs	ν(C5=C6); β(NH₂), ν(COO⁻)
1566 m	1554 m	1560 m	1568 m	δ_{ip}(N1H1, N5H5); ν(C5C6), β_s(NH₂)
1511 w	1506 m	1492 w/m	1501 w	δ(NC); ν(ring); δ_{ip}(N3H3)
1457 m		1447 w	1437 w	ν(ring), β_s(NH₂), δ(Nl–H1), ν(COO⁻)
1436 m	1408 s	1421 w	1414 vs	δ(N3H3), δ(ring), δ(N1H1)
1405 m	1377 s		1351 s	δ(N3H3), δ(ring), δ(N1H1), ν_s(COO⁻)
1312 m	1309 m	1301 w	1310 m/s	ν(C5–N), ν(C–N), δ(OH), β_s(NH₂)
1255 m/s	1276 sh			ν(C–N), δ(N1H1), r(NH₂), δ(ring)
1234 m/s	1236 w	1242 m	1250 m/s	ν(C–N), δ(N3H3), r(NH₂), δ(NlH1)
1140 sh	1130 vw		1122 vw	δ(OH)
1083 vw	1060	1047 vw	1052 w	ν(C6-O, C6-C7), β_{as}(NH₂)
989 sh				ν(NCN), δ(N3H3), r(NH₂), δ(NlH1)
924 w	941 sh	919 w/m	927 w/m	ν(NCC), ν(ring), r(NH₂), ν(COO)
871 w/m	874 vw			γ(N3–H3), γ(ring)
795 vw	825 m	809 vw	789 m	δ_{op}(O3C7O1)
767 vw	794 w		765 sh	γ(C4=O4), γ(C4–C=C6), γ(C6–C12)
754 w	752 w	748 vw		γ(C6–C12), γ(C4=O4), γ(COOH), γ(N3–H)
740 w	719 w		714 m	γ(C2=O2), γ(NC2N), γ(N3–H)
696 vw	694 vw			δ(ring), Δ_sCOO), r(NH₂)
	611 vw			ν(Ho-O)
584 vw	592 vw	582 w	595 w/m	δ(ring), Δ_s(COO)
	509 sh			ν(Ho-O)
488 w	499 w	482 w/m	491 m	δ(ring), δ(NH₂), Δ_s(COO)
474 w/m	468 sh			γ(OH)
446 m	443 m	445 w	454 m	δ(OCNCO), δ(COO) + r(NH₂)
	424 sh	425 sh	435 w/sh	τ(C2O2, ring), Δ_{as}(COO)
		381 vw	365 w	δ(OCCN11), δ(COO), δ(C2=O), r(NH₂); ν(Ho-O)
		249 w	255 w	τ(NH₂), Δ_s(COO)
			207 w	ν(O-Ho-O)
		196 w	197 sh	τ(ring); δ(O-Ho-O)

Abbreviation: vw – very weak; w – weak; m – medium; ms – medium strong; s – strong; vs – very strong; sh – shoulder; ν – stretching; δ – bending; τ – torsion; s– symmetric; as– asymmetric; def. – deformation; ip – in plane; op – out of plane; ring – pyrimidine ring; sciss – scissoring

The spectra in the frequency region below 600 cm⁻¹ are particularly interesting, since they provide information about the metal-ligand vibrations. The new band at 611 cm⁻¹ and the new shoulder at 509 cm⁻¹ present only in the IR spectrum of the complex, which cannot be observed in its Raman spectrum, can be due to the Ho-O interactions [38, 58-59]. In the Raman low wavenumbers region of the complex (Figure 3), the band that can be due to the Ho-O vibrations [38], is the band at 365 cm⁻¹. Besides the appearance of a new shoulder at 424 cm⁻¹ in the IR spectrum of the ligand confirm the presence of the Ho-O interaction. The metal affects not only the carboxylate anion but also the ring structure. Usually the carboxylic acids interact with the metals as symmetric, bidentate carboxylate anions and both oxygen atoms of the carboxylate are symmetrically bonded to the metal. In this sense, we can observe in the Raman spectrum of the Ho(III) complex a weak peak at 207 cm⁻¹, which can be due to the O1-Ho-O3 vibration modes (Table 1) [38, 58]. The Raman spectra are particularly useful in studying the metal-oxygen stretching vibrations, since these vibrations give rise to medium intensity bands in Raman, but are weak in the infrared spectra. The detailed assignment of the remaining bands in the vibrational spectra is shown in Table 1.

Therefore, on the basis of the experimental and theoretical results, we were able to suggest that in the Ho(III) complex studied, the metal ion coordinated to the carboxylic oxygen atoms, as it is shown in Figure 4.
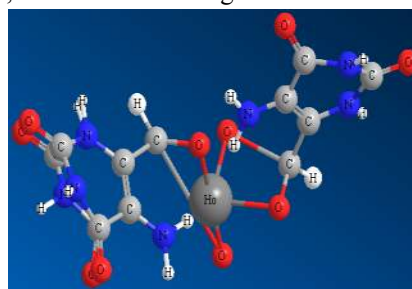

Figure 4. Suggested metal–ligand coordination in the investigated Ho(III) complex.

3.3. Pharmacology.

3.3.1. Effects of HAOA and HoAOA on isolated rat liver microsomes.

One of the most suitable sub-cellular *in vitro* systems for investigation of drug metabolism is isolated microsomes. Administered alone, HAOA and HoAOA, didn't reveal statistically significant toxic effects on isolated rat microsomes. The level of malondialdehyde (MDA), marker for lipid peroxidation, was not increased statistically significant from both HAOA and HoAOA, compared to the control (non-treated microsomes) (Figure 5).
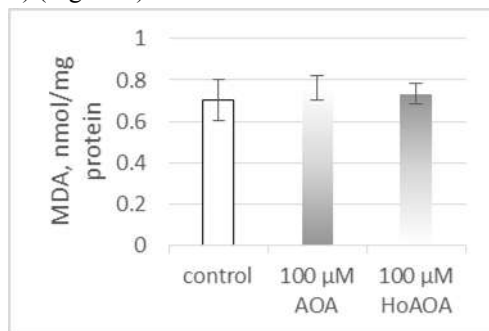

Figure 5. Effects of 100 μM HAOA and HoAOA, administered alone, on isolated rat microsomes.

In conditions of non-enzyme-induced lipid peroxidation, the examined compounds HAOA and HoAOA, revealed statistically significant antioxidant activity, compared to toxic agent – Fe^{2+}/AA (iron/ascorbate). The antioxidant effect was most prominent for the complex HoAOA (Figure 6).

Microsomes incubation with Fe^{2+}/AA, resulted in statistically significant increase of the amount of MDA with 191 % vs control (non-treated microsomes). In non-enzyme-induced lipid peroxidation model, pre-treatment with HAOA and HoAOA

at concentration 100 μM, significantly reduced lipid damage by 44 and by 70 %, respectively, as compared to the toxic agent (Fe^{2+}/AA) (Figure 6). The antioxidant effect was most prominent in pre-treatment with the complex HoAOA.
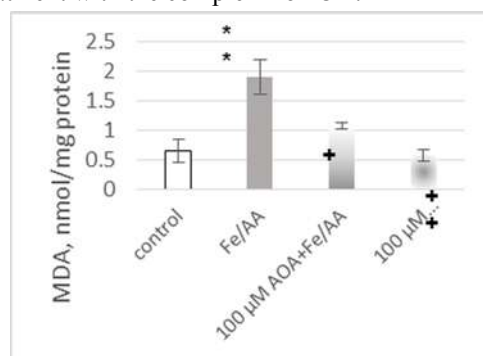

Figure 6. Effects of 100 μM HAOA and HoAOA, in non-enzyme-induced lipid peroxidation, on isolated rat microsomes.

** $P < 0.01$ vs control (non-treated microsomes)

+ $P < 0.05$; ++ $P < 0.01$ vs toxic agent (Fe^{2+}/AA)

3.3.2. Effects of HAOA and HoAOA on isolated rat liver hepatocytes.

In vitro studies are suitable for assessing new perspective compounds. The perspective new compounds, with proved pharmacological activity and predictable hepatic metabolism, must be examined for cyto- and hepatotoxicity. Convenient, well-controlled biological model systems with high drug-metabolizing capacities, which can be used in experimental toxicology, are isolated rat hepatocytes.

Administered alone, the compounds HAOA and HoAOA, revealed statistically significant cytotoxic effects on freshly isolated rat hepatocytes. The cytotoxicity of the complex HoAOA was lower than those of HAOA (Table 2).

Table 2. Effects of 100 μM HAOA and HoAOA, administered alone, on parameters, characterizing the functionally-metabolizing capacity of isolated rat hepatocytes

Group	Cell viability, %	LDH leakage, μmol/min/10^6 cells	GSH level, nmol/10^6 cells	MDA level, nmol/10^6 cells
Control	89 ± 3.5	0.115 ± 0.01	20 ± 3.1	0.055 ± 0.01
100 μM HAOA	66 ± 4.1 **	0.253 ± 0.01 **	15 ± 2.2 *	0.110 ± 0.01 **
100 μM HoAOA	70 ± 3.3 **	0.234 ± 0.01 **	16 ± 2.4 *	0.103 ± 0.01 **

* $P < 0.05$; ** $P < 0.01$ vs control (non-treated hepatocytes)

HAOA decreased the cell viability (measured by Trypan blue exclusion) and level of reduced glutathione (GSH) with 26 % and 25 %, respectively; and increased lactate dehydrogenase (LDH) leakage and MDA production with 120 % and 100 %, compared to the control (non-treated hepatocytes) (Table 2).

HoAOA decreased the cell viability and level of GSH with 21 % and 20 %, respectively; and increased LDH leakage and MDA production with 103 % and 87 %, compared to the control (non-treated hepatocytes) (Table 2).

The microsomal fraction, which is prepared by differential centrifugation, contents fragments from the endoplasmatic reticulum and preserve the enzyme activity, mostly cytochrome P450 enzymes. Microsomes are used as a model of lipid membrane in experiments, related to the process of lipid

peroxidation [60]. Here, we show that HAOA and HoAOA revealed statistically significant antioxidant effect in non-enzyme-induced lipid peroxidation in isolated microsomes. The antioxidant effects were more prominent in the complex HoAOA compared to the ligand HAOA. These effects of HoAOA might be due to the presence of Ho(III) ions in the complex.

In experimental toxicology, the in vitro systems are widely used for the investigation of the xenobiotics biotransformation, and for revealing the possible mechanisms of toxic stress and its prevention. Isolated liver cells are a convenient model system for evaluation of the cytotoxic and cytoprotective effects of some promising biologically active compounds both newly synthesized and derived from plants. On isolated rat hepatocytes, both HAOA and HoAOA revealed statistically

significant cytotoxic effects, but the complex HoAOA showed lower cytotoxicity than the ligand HAOA. This lower cytotoxicity might be due to the complexation process and to the influence of Ho(III) ions.

4. CONCLUSIONS

The coordination ability of HAOA was proved in complexation reaction with Ho(III) ions. The newly synthesized Ho(III) complex of 5-aminoorotic acid has been characterized by elemental and spectral (IR, Raman) analyses. IR and Raman spectra of 5-aminoorotic acid and its Ho(III) complex were recorded and the marker bands of characteristic functional groups were identified, in order to use them as data bank for further application in trace analysis of rare-earth complexes. The vibrational studies and the previous density functional calculations revealed that the most probable binding of the ligand to Ho(III) ions is bidentate through the deprotonated carboxylic oxygen atoms. Therefore, the theoretical and spectral studies helped to explain the vibrational behaviour of the ligand and gave evidence for its coordination mode to Ho(III) ions. The obtained results were in good agreement with the other literature studies and theory predictions.

According to our expectations the Ho(III) complex as other investigated earlier by us lanthanide(III) complexes possesses antioxidant activity and its effects are clearly expressed. The antioxidant effects were more prominent in the complex HoAOA compared to the ligand HAOA and this observation might be due to the presence of Ho(III) ions in the complex. The lower cytotoxicity of the complex HoAOA might be also due to the complexation process and to the influence of Ho(III) ions. Taken together the results from the pharmacology screening give us reason to conclude that the Ho(III) complex with 5-aminoorotic acid necessitates further more detailed pharmacological evaluation. These results confirmed our previous observations on the cytotoxicity of lanthanide(III) complexes with other biologically active ligands.

5. REFERENCES

[1] Panzeter P.L., Ringer D.P., DNA precursors are channelled to nuclear matrix DNA replication sites, *Biochem. J.*, 293, 775–779, **1993**.

[2] Berthelot M., Cornu G., Daudon M., Helbert M., Laurence C., Computer-aided infrared analysis of urinary calculi, *Clin. Chem.*, 33, 2070–2073, **1987**.

[3] Banditt P.J., Determination of orotic acid in serum by high-performance liquid chromatography, *J. Chromatogr. B.*, 660, 176–179, **1994**.

[4] MacCann M.T., Thompson M.M., Gueron I.C., Tuchman M., Quantification of orotic acid in dried filter-paper urine samples by stable isotope dilution, *Clin. Chem.*, 41, 739–743, 1995.

[5] Sarpotdar A., Burr G.J., The structures and hydrogen ion dependence of the complexes between orotic acid derivatives and the ions, Ni(II) and Eu(III), *J. Inorg. Nucl. Chem.*, 41, 549–553, **1979**.

[6] Lalart D., Dodin G., Dubois J.E., Study of the slow protonation of the complexes between divalent nickel ion and dianion of orotic-acid or its derivatives, *J. Chim. Phys.*, 79, 449–453, **1982**.

[7] Bach I., Kumberger O., Schmidbaur H., Orotate complexes. Synthesis and crystal structure of lithium orotate (-I) monohydrate and magnesium bis [orotate (-I)] octahydrate, *Chem. Ber.*, 123, 2267–2271, **1990**.

[8] Kumberger O., Riede J., Smidbaur H., Orotate complexes, II1) preparation and crystal structures of calcium and zinc orotate (2-) hydrates, *Chem. Ber.*, 124, 2739–2742, **1991**.

[9] Baran E.J., Mercader R.C., Hueso-Urena F., Moreno-Carretero M., Quiro´s-Olozabal M., Salas-Peregrin J. M., Crystal structure, raman and ^{57}Fe mossbauer spectra of the Fe II complex of iso-orotic acid, *Polyhedron*, 15, 1717–1721, **1996**.

[10] Fernandez Garcıa E., McGregor J.U., Determination of organic acids during the fermentation and cold storage of yogurt, *J. Dairy Sci.*, 77, 2934–2939, **1994**.

[11] Akalin A.S., Gone S., The determination of orotic acid in ruminant milks using HPLC, *Milchwissenschaft*, 51, 554–556, **1996**.

[12] Ruasmadiedo P., Badagancedo J.C., Fernandez Garcia E., Dellano D.G., de los Reyes Gavilan C. G., Preservation of the microbiological and biochemical quality of raw milk by carbon dioxide addition: A pilot-scale stud, *J. Food Protect*, 59, 502–508, **1996**.

[13] Takusawaga F., Shimada A., The crystal structure of orotic acid monohydrate (vitamin B 13), *Bull. Chem. Soc. Jpn.*, 46, 2011–2019, **1973**.

[14] Elroby S.A., Electronic structure of orotic acid II: Acidity, basicity, and interaction with water. *J. Mol. Str.: THEOCHEM*, *803*, 67-72, 2007.

[15] Letellier R., Ghomi M., Taillandier E., Out-of-plane vibration modes of nucleic acid bases, *Eur. Biophys. J.*, 14, 243–252, **1987**.

[16] Person W. B., Szczepaniak K., In *Vibrational Spectra and Structure* (Ed.: J. R. Durig), Elsevier, Amsterdam, pp. 239–325, **1993**.

[17] Rostkowska H., Szczepaniak K., Nowak M.J., Leszczynski J., Kubulat K., Person W.B., Thiouracils. 2. Tautomerism and infrared spectra of thiouracils. Matrix-isolation and ab initio studies, *J. Am. Chem. Soc.*, 112, 2147–2160, **1990**.

[18] Gould I.R., Hillier I.H., Accurate calculations of the oxo–hydroxy tautomers of uracil, *J. Chem. Soc. Perkin Trans*, 2, 329–330, **1990**.

[19] Leszczynski J., Tautomerism of uracil: the final chapter? Fourth-order electron correlation contributions to the relative energies of tautomers, J. *Phys. Chem.*, 96, 1649–1653, **1992**.

[20] Thomas Jr. G.J., Tsuboi M., In *Advances in Biophysical Chemistry*, Bush, C.A., Ed., JAI Press: Greenwich, CT, pp. 1–70, **1993**.

[21] Florian J., Hrouda V., Scaled quantum mechanical force fields and vibrational spectra of solid state nucleic acid constituents V: thymine and uracil, *Spectrochim. Acta*, 49A, 921–938, **1993**.

[22] Lagant P., Vergoten G., Efremov R., Peticolas W.L., Normal coordinate treatment of 1-methylthymine in the crystalline state: Use of the ultraviolet resonance Raman intensities to improve the vibrational force field, *Spectrochim. Acta.*, 50A, 961–971, **1994**.

[23] Peticolas W.L., Rush T., Ab initio calculations of the ultraviolet resonance Raman spectra of uracil, *J. Comput. Chem.*, 16, 1261–1270, **1995**.

[24] Rush T., Peticolas W.L., Ab initio transform calculation of resonance raman spectra of uracil, 1-methyluracil, and 5-methyluracil, *J. Phys. Chem.*, 99, 14647–14658, **1995**.

[25] Aamouche A., Berthier G., Coulombeau C., Flament J.P., Ghomi M., Henriet C., Jobic H., Turpin P.Y., Molecular force fields of uracil and thymine, through neutron inelastic scattering experiments and scaled quantum mechanical calculations, *Chem. Phys.*, 204, 353–363, **1996**.

[26] Aamouche A., Ghomi M., Coulombeau C., Jobic H., Grajcar L., Baron M. H., Baumruk V., Turpin P. Y., Henriet C., Berthier G. J., Neutron inelastic scattering, optical spectroscopies and scaled quantum mechanical force fields for analyzing the vibrational dynamics of pyrimidine nucleic acid bases. 1. Uracil, *J. Phys. Chem.*, 100, 5224–5234, **1996**.

[27] Aamouche A., Ghomi M., Coulombeau C., Grajcar L., Baron M. H., Jobic H., Berthier G., Neutron inelastic scattering, optical spectroscopies, and scaled quantum mechanical force fields for analyzing the vibrational dynamics of pyrimidine nucleic acid bases. 2. Thymine, *J. Phys. Chem. A.*, 101, 1808–1817, **1997**.

[28] Maistralis G., Koutsodimou A., Katsaros N., Transition metal orotic acid complexes, *Transit. Met. Chem.*, 25, 166-173, **2000**.

[29] Nepveu F., Gaultier N., Korber N., Jaud J., Castan P., New polynuclear manganese (II) complexes with orotic acid and some of its derivatives: crystal structures, spectroscopic and magnetic studies, *J. Chem. Soc. Dalton Trans.*, 24, 4005-4014, **1995**.

[30] Tucci E.R., Doody B.E., Li N.C., Acid dissociation constants and complex formation constants of several pyrimidine derivatives, *J. Phys. Chem.*, 65, 1570-1574, **1961**.

[31] Tucci E.R., Ke C.H., Li N.C., Linear free energy relationships for proton dissociation and metal complexation of pyrimidine acids, *J. Inorg. Nucl. Chem.*, 29, 1657-1667, **1967**.

[32] Sabat M., Zglinska D., Jezowska-Trzebiatowska B., Tetraaquaorotatonickel (II) monohydrate, *Acta Crystallogr. B*, 36, 1187-1188, **1980**.

[33] Mutikainen I., Lumme P., The structure of diammine (orotato) copper (II), *Acta Crystallogr. B*, 36, 2233-2237, **1980**.

[34] Solin T., Matsumoto K., Fuwa K., The crystal structure of cis-diammine (orotinato) platinum (II), *Bull. Chem. Soc. Jpn.*, 54, 3731-3734, **1981**.

[35] Khodashova T.S., Davidenko N.K., Vlasova N.N., Crystalline and molecular-structure of various-ligand copper (II) complex with glycinate and orotate, *Koord. Khim.*, 10, 262-268, **1984**.

[36] Karipides A., Thomas B., The structures of tetraaqua (uracil-6-carboxylate) zinc (II) monohydrate (A) and tetraaqua (uracil-6-carboxylato) nickel (II) monohydrate (B), *Acta Crystallogr. C*, 42, 1705-1707, **1986**.

[37] Mutikainen I., Polymeric metal-orotato complexes-the crystal and molecular-structure of $[(C_5H_2N_2O_4)Co(H_2O)[OH](NH_3)]_n$ and $[(C_5H_2N_2O_4)Ni(H_2O)_2(NH_3)]_n$ formed between Co(III) and Ni(II) and orotato-anion, *Finn. Chem. Lett.*, 5, 193-200, **1985**.

[38] Kostova I., Peica N., Kiefer W., Theoretical and spectroscopic studies of lanthanum (III) complex of 5-aminoorotic acid, *Chem. Phys.*, 327, 494-505, **2006**.

[39] Kostova I., Manolov I., Konstantinov S., Karaivanova M., Synthesis, physicochemical characterisation and cytotoxic screening of new complexes of cerium, lanthanum and neodymium with Warfarin and Coumachlor sodium salts, *Eur. J. Med. Chem.*, 34, 63-68, **1999**.

[40] Kostova I., Manolov I., Nicolova I., Danchev N., New metal complexes of 4-methyl-7-hydroxycoumarin sodium salt and their pharmacological activity, *Il Farmaco*, 56, 707-713, **2001**.

[41] Kostova I., Manolov I., Nicolova I., Konstantinov S., Karaivanova M., New lanthanide complexes of 4-methyl-7-hydroxycoumarin and their pharmacological activity, *Eur. J. Med. Chem.*, 36, 339-347, **2001**.

[42] Kostova I., Manolov I. I., Radulova M. K., Stability of the complexes of some lanthanides with coumarin derivatives. I. Cerium (III)-4-methyl-7-hydroxycoumarin, *Acta Pharm.*, 54, 37-47, **2004**.

[43] Kostova I., Manolov I. I., Radulova M. K., Stability of the complexes of some lanthanides with coumarin derivatives. II. Neodymium (III)-acenocoumarol, *Acta Pharm.*, 54, 119-131, **2004**.

[44] Kostova I., Manolov I. I., Momekov G., Cytotoxic activity of new neodymium (III) complexes of bis-coumarins, *Eur. J. Med. Chem.*, 39, 765-775, **2004**.

[45] Kostova I., Trendafilova N., Momekov G., Theoretical and spectroscopic evidence for coordination ability of 3, 3′-benzylidenedi-4-hydroxycoumarin. New neodymium (III) complex and its cytotoxic effect, *J. Inorg. Biochem.*, 99, 477-487, **2005**.

[46] Kostova I., Momekov G., Zaharieva M., Karaivanova M., Cytotoxic activity of new lanthanum (III) complexes of bis-coumarins, *Eur. J. Med. Chem.*, 40, 542-551, **2005**.

[47] Kostova I., Kostova R., Momekov G., Trendafilova N., Karaivanova M., Antineoplastic activity of new lanthanide (cerium, lanthanum and neodymium) complex compounds, *J. Trace Elem. Med. Biol.*, 18, 219-226, **2005**.

[48] Kostova I., Trendafilova N., Mihailov T., Theoretical and spectroscopic studies of pyridyl substituted bis-coumarins and their new neodymium (III) complexes, *Chem. Phys.*, 314, 73-84, **2005**.

[49] Deby C., Goutier R., New perspectives on the biochemistry of superoxide anion and the efficiency of superoxide dismutases, *Biochem. Pharmacol.*, 39, 399-405, **1990**.

[50] Lowry O. H., Rosebrough N. J., Farr A. L., Randal R. J., Protein measurement with the Folin phenol reagent, *J. Biol. Chem.*, 193, 265-275, **1951**.

[51] Kim H.J., Chun Y.J., Park J.D., Kim S.I., Roh J.K., Jeong T.C., Protection of rat liver microsomes against carbon tetrachloride-induced lipid peroxidation by red ginseng saponin through cytochrome P450 inhibition, *Planta Med.*, 63, 415-418, **1997**.

[52] Mitcheva M., Kondeva M., Vitcheva V., Nedialkov P., Kitanov G., Effect of benzophenones from Hypericum annulatum on carbon tetrachloride-induced toxicity in freshly isolated rat hepatocytes, *Redox Rep.*, 11, 3-8, **2006**.

[53] Fau D., Berson A., Eugene D., Fromently B., Fisch C., Pessayre D., Mechanism for the hepatotoxicity of the antiandrogen, nilutamide. Evidence suggesting that redox cycling of this nitroaromatic drug leads to oxidative stress in isolated hepatocytes, *J. Pharmacol. Exp. Ther.*, 263, 69-77, **1992**.

[54] Oh K.Y., Roberts V.H., Schabel M.C., Grove K.L., Woods M., Frians A.E., Gadolinium chelate contrast material in pregnancy: Fetal biodistribution in the nonhuman primate, *Radiology*, 276, 110-118, **2015**.

[55] Hambley T.W., Christopherson R. I., Zvargulis E. S., Models of the active site of dihydroorotase: structure of diaquabis (L-dihydroorotato) zinc (II) reveals an unexpected coordination mode for the L-dihydroorotato ligands, *Inorg. Chem.*, 34, **6550-6552, 1995**.

[56] Perlepes S.P., Lazaridou V., Sankhla B., Tsangaris J. M., Synthesis, physical properties and spectroscopic studies of isoorotato, 5-aminoorotato and 2-thioorotato lanthanide (III) complexes, *Bull. Soc. Chim. Fr.*, 127, 597-608, **1990**.

[57] Lalioti N., Raptopoulou C.P., Terzis A., Panagiotopoulos A., Perlepes S. P., Manessi-Zoupa E., New metal-binding modes for 5-aminoorotic acid: preparation, characterization and crystal structures of zinc (II) complexes, *J. Chem. Soc., Dalton Trans.*, 1327–1333, **1998**.

[58] Gelfand L.S., Iaconianni F.J., Pytlewski L.L., Speca A.N., Mikulski C.M., Karayannis N.M., Nicotinic and isonicotinic acid n-oxide interactions with 3d metal perchlorates, *J. Inorg. Nucl. Chem.*, 42, 377-385, **1980**.

[59] Nakamoto K., *Infrared and Raman spectra of inorganic and coordination compounds Part B*, Fifth Ed, Wiley, New York, **1997**.

[60] Zaidi S.I., Agarwal R., Eichler G., Rihter B.D., Kenney M.E., Mukhtar H., Photodynamic effects of new silicon phthalocyanines: in vitro studies utilizing rat hepatic microsomes and human erythrocyte ghosts as model membrane sources, *Photochem. Photobiol.*, 58, 204-210, **1993**.

6. ACKNOWLEDGEMENTS